Neurotransmitters Drive Combinatorial Multistate Postsynaptic Density Networks

Published in final edited form as:
Sci Signal. ; 2(68): ra19. doi:10.1126/scisignal.2000102.

Neurotransmitters Drive Combinatorial Multistate Postsynaptic Density Networks

Marcelo P. Coba[1], **Andrew J. Pocklington**[2], **Mark O. Collins**[3], **Maksym V. Kopanitsa**[1], **Rachel T. Uren**[1], **Sajani Swamy**[3], **Mike D. R. Croning**[1], **Jyoti S. Choudhary**[3], and **Seth G. N. Grant**[1,*]

[1]Genes to Cognition, Wellcome Trust Sanger Institute, Hinxton, Cambridgeshire CB10 1SA, UK.

[2]Institute for Adaptive and Neural Computation, Division of Informatics, University of Edinburgh, 5 Forrest Hill, Edinburgh EH1 2QL, UK.

[3]Proteomic Mass Spectrometry, Wellcome Trust Sanger Institute, Hinxton, Cambridgeshire CB10 1SA, UK.

Abstract

The mammalian postsynaptic density (PSD) comprises a complex collection of ~1100 proteins. Despite extensive knowledge of individual proteins, the overall organization of the PSD is poorly understood. Here, we define maps of molecular circuitry within the PSD based on phosphorylation of postsynaptic proteins. Activation of a single neurotransmitter receptor, the *N*-methyl-D-aspartate receptor (NMDAR), changed the phosphorylation status of 127 proteins. Stimulation of ionotropic and metabotropic glutamate receptors and dopamine receptors activated overlapping networks with distinct combinatorial phosphorylation signatures. Using peptide array technology, we identified specific phosphorylation motifs and switching mechanisms responsible for the integration of neurotransmitter receptor pathways and their coordination of multiple substrates in these networks. These combinatorial networks confer high information processing capacity and functional diversity on synapses and their elucidation may provide new insights into disease mechanisms and new opportunities for drug discovery.

INTRODUCTION

The vertebrate PSD, the specialized region at which one neuron receives electrical input from another, is strikingly complex, consisting of over 1000 proteins. Understanding the functional architecture of the molecular networks formed by these synaptic proteins is critical to understanding how neurons transmit and process information.

Excitatory synapses of the mammalian hippocampus exhibit structural and functional plasticity thought to underlie the processes of learning, memory, and various behaviors (1). The *N*-methyl-D-aspartate–type glutamate receptor (NMDAR) participates in complexes with scaffold proteins and various other molecules (2–5). Activation of NMDARs is known to modulate the activity of postsynaptic tyrosine, serine, and threonine kinases (1, 6), and it has become increasingly clear that hundreds of phosphorylation sites on many classes of proteins exist (1, 7–9). Although it is not known whether these phosphorylation sites are organized into signaling networks of many highly interconnected proteins, computational models support the view that synaptic signaling networks are advantageous over traditional simpler biochemical models that utilize few molecular steps in simple pathways (10, 11). These advantages include improved storage and retention of memories (12, 13). Although recent studies have modeled synapse proteome interaction networks in the postsynaptic terminal (14, 15) and cannabinoid receptor–driven neuronal transcription factor networks (16), the signaling networks in the PSD are poorly defined.

Europe PMC Funders Author Manuscripts

Here, we report the mapping of postsynaptic phosphoproteome signaling networks with the use of a combination of in vivo, in vitro, and computational approaches. These phosphoproteome networks show that a single neurotransmitter receptor integrates hundreds of downstream postsynaptic events into a network that overlaps with those driven by other neurotransmitter receptors. The networks show multiple levels of organization and contain building blocks of components that assemble the molecular circuitry of synapse signaling. This organization into molecular circuits has important implications for the basic mechanisms of learning and disease and its elucidation opens new avenues for drug discovery in the brain.

RESULTS

Neurotransmitter receptors drive overlapping postsynaptic proteome networks that modulate protein phosphorylation status

The NMDAR was stimulated in mouse hippocampus brain slices by bath application of NMDA, a protocol that induces long-term depression (LTD) (17). The phosphorylation of PSD proteins was quantified by liquid chromatography–tandem mass spectrometry (LC-MS/MS). Three minutes of exposure to NMDA elicited changes in the phosphorylation status of 127 proteins (Fig. 1A) and 189 phosphopeptides (tables S1–S3); the phosphorylation of 41phosphorylated peptides showed no significant change. Phosphorylation increased on 44 peptides (23%) from 38 proteins (28%) and decreased on 145 (77%) peptides from 101 proteins (79%) indicating the simultaneous regulation of kinases and phosphatases These substrate proteins were members of a wide range of functional classes: Channels and receptors accounted for 10% of all modulated proteins; these included some implicated in fast synaptic transmission [e.g., the GluR2 subunit of the ionotropic AMPA (α-amino-3-hydroxy-5-methyl-4-isoxazolepropionic acid) receptor] and excitability (e.g., voltage-gated K^+ channels) and some implicated in slower processing pathways (e.g., Ca^{2+} channels and the metabotropic G protein–coupled glutamate receptor 5, mGluR5). Structural components (scaffolding proteins, cytoskeletal proteins, and proteins involved in cell adhesion) accounted for 30% of all modulated proteins, whereas proteins implicated in transcription and translation accounted for ~15%. This last group was largely split between proteins mediating pre–messenger RNA splicing (60%) and transcription (33%). These data indicate that NMDAR stimulation activates a signaling network that modulates the phosphorylation status of >100 postsynaptic proteins, thereby influencing diverse functional processes.

Of 540 members of the total mouse kinome (18), ~50 kinases are found in the PSD (4, 19, 20). We measured the NMDAR-dependent activation of 23 PSD kinases (Fig. 1, B and C) at 3, 20, and 40 min after NMDA application, using immunoblotting with phosphospecific antibodies. Nine PSD kinases (39% of those tested) showed changes in phosphorylation status, with 7 showing increased phosphorylation and 2 showing decreased phosphorylation. The peak change was detected at 3 min after NMDA treatment and phosphorylation status had returned to baseline by 40 min. The 9 modulated kinases included representatives of four major kinase groups: AGC (protein kinase A, protein kinase G, and protein kinase C, PKA-PKG-PKC), CMGC [cyclin-dependent kinases (CDKs), mitogen-activated protein kinases (MAPKs), glycogen synthesis kinases (GSKs), and CDK-like kinases], STE (sterile-phenotype kinases), and PTK (protein tyrosine kinase). Together with the MS data, these indicate that NMDAR activation simultaneously modulates the activity of multiple kinases (in various classes), leading to changes in the phosphorylation status of numerous substrates.

Metabotropic glutamate receptors (mGluRs) and dopamine receptors physically interact with NMDAR in postsynaptic complexes, and their activation also modulates synaptic plasticity and behavior. Using phosphospecific antibodies, we treated hippocampal slices with specific receptor agonists [NMDA to activate NMDAR, 3,5-dihydroxyphenylglycine (DHPG) to

activate mGluR, and the dopamine receptor D1 agonist 6-chloro-7,8-dihydroxy-1-phenyl-2,3,4,5-tetrahydro-1*H*-3-benzazepine (6-Cl-PB)], extracted proteins, and assessed phosphorylation of 10 sites on four glutamate receptor subunits (Fig. 2 and table S4). Stimulation of these receptors elicited distinct but overlapping changes in the phosphorylation status of these 10 sites. Similarly, activation of dopamine and glutamate receptors, treatments that are known to stimulate PKA and PKC activity (23, 24), produced overlapping profiles in the 10 sites, showing further combinations in the postsynaptic phosphorylation network.

Because these neurotransmitter receptors are the targets for therapeutic drugs, our results open the possibility that the phosphorylation networks they activate may include disease-relevant proteins. Of the NMDA-modulated proteins, 21 are implicated in the pathology of Alzheimer's (AD), Parkinson's, and Huntington's diseases, schizophrenia, or autism (table S5). Moreover, reflecting the overlap in their corresponding networks, drugs that modulate NMDA receptor, mGluR, or dopamine receptor function are useful in treating the symptoms of this set of diseases (21–28).

Phosphoproteome building blocks

In its simplest form, the addition or removal of a phosphate residue is a fundamental binary switch that changes the properties of a protein (29). To understand how a signaling network is organized, it is necessary to build a phosphoproteome network that includes information on the kinases that phosphorylate specific sites. We classified a set of "minimal building blocks" representing fundamental regulatory motifs (analogous to types of switches) that can be assembled to produce a molecular circuitry of the postsynaptic proteome (Fig. 3, A to G).

This set of regulatory motifs represents both phosphorylation events that occur on single phosphorylation sites (Fig. 3A) and those that involve multiple phosphorylation sites (where the phosphoacceptors are within 10 amino acid residues) (Fig. 3B). Of 610 known in vivo phosphorylation sites present in 92 synaptic proteins (7), 383 (63%) occurred within 10 amino acids of another, indicating that both types of sites are common (tables S6, S7, and S8). Considering single-site substrates, a single kinase may phosphorylate multiple independent sites (kinase divergence motif; Fig. 3C) or multiple kinases can phosphorylate a common site (kinase convergence motif; Fig. 3D). Considering two adjacent-site substrates (as the simplest version of multiple sites), each site can be independently phosphorylated (paired convergence motif, Fig. 3, E and F) or priming or interference between pairs can occur when the phosphorylation of the first site in the pair influences the phosphorylation of the second site (primed convergence motif; Fig. 3G).

To map the distribution of these building blocks onto known phosphorylation sites in the postsynaptic proteome, we constructed peptide arrays comprising these sites and assayed phosphorylation by specific kinases. A postsynaptic phosphoproteome array (PPParray), with 600 peptides corresponding to 300 in vivo phosphorylation sites on 92 synaptic proteins, was constructed from in vivo phosphorylation sites modulated by NMDA, large-scale synapse phosphoproteomic studies (7), or individual publications (tables S6, S9, and S10). Peptides were immobilized on glass slides, together with their corresponding control (in which the serine, threonine, or tyrosine phosphoacceptor sites were substituted with alanine, valine, or phenylalanine, respectively) (Fig. 3H). Positive control peptides containing consensus sequences for specific kinases were included. The classes of proteins represented included receptors, scaffolding proteins, enzymes, cytoskeletal proteins, and others.

Twenty-five postsynaptic kinases (table S11) with representatives from all major families in the mouse kinome were used to phosphorylate the PPParray (Fig. 3H). Phosphorylation was

regarded as positive if reproduced in triplicate and detected above background of negative controls (table S12). A total of 723 phosphorylation events (kinase phosphorylation of a site) were detected, involving all 25 kinases and 77 (84%) of the 92 proteins. Of the 300 sites assayed, 166 (55%) were phosphorylated (471 events) (table S13). We also detected the phosphorylation of 36 other specific sites (94 events), of which 30 were previously undescribed in vitro sites (table S7). A further 158 events on 58 sequences where the specific site could not be unambiguously determined (because there were 2 or more potential phosphoacceptor sites) were also detected (table S14). We created a Web resource that provides access to these data and provides links to physiological and behavioral data from knockout mice as well as disease data for the respective kinases and substrates (www.genes2cognition.org/phosphoproteomics/coba1/).

All kinases and substrates studied were localized in the PSD and we further examined the kinase-site assignment in vivo. In addition to our experiments with phosphospecific antibodies and kinase manipulations in hippocampal slices (described below), we mined the literature for relevant data. Overall, of the 166 sites phosphorylated by 25 kinases in the PPParray, we found in vivo validation for 78 (47%) sites by 14 (56%) kinases (tables S6 and S8). We extended these validation data with additional experiments testing the kinase assignments to specific sites on key synaptic proteins implicated in synaptic plasticity: kinases; ERK2 (extracellular signal–regulated kinase 2) (30), PKA (31), GSK3 (32), and CaMKII (calcium- and calmodulin-dependent protein kinase) (33); substrates for phosphorylation—PSD95 (34), the NR2B subunit of the NMDR (35), and GluR1 (36). These examples indicate that the assignment of kinases to known in vivo sites (discovered using MS) using peptide arrays provides reliable validation of kinase-substrate identifications (fig. S1). Furthermore, in vivo data from other laboratories provided additional prospective validation of novel PPParray assignments during the course of our experiments, tyrosine phosphorylation of NR2B Tyr^{1304};Calpain-1 site Tyr^{387} (www.phosphosite.org), and GluR1 Thr^{840} (37)(Thr^{858} in (8, 37) were described in vivo following their in vitro discovery.

Postsynaptic phosphoproteome networks

Figure 4, which shows the kinase-substrate network with annotations of functional classes and regulatory motifs, illustrates the complexity ofsynaptic phosphorylation and widespread distribution of switching mechanisms. Note that this diagram underrepresents the scale of phosphorylation because individual sites are not shown within the substrates. Moreover, this network would be expected to increase in density if further postsynaptic kinases and substrates were tested. We therefore consider this a draft map of the synapse phosphoproteome network that allows us to identify general principles of its organization and function.

We next examined the distribution of phosphorylation events (Fig. 5A). Individual serine, threonine, or tyrosine kinases phosphorylated between 5 and 56 sites, with an average of 29 sites per kinase (a pattern characterized as the kinase divergence motif; Fig. 3C). These phosphorylation sites were distributed over 4 to 36 protein substrates, with an average of 21 substrates phosphorylated by a single kinase. To investigate the range of cell biological processes influenced by each kinase, substrates were assigned to broad functional families, including ion channels and receptors, scaffolding proteins, cytoskeletal proteins, and others (table S9). The substrates of a kinase were typically drawn from a wide range of families. For instance, PKA phosphorylated 29 substrates from 9 families and ERK2 phosphorylated 36 substrates from 8 families. Phosphoinositide-dependent kinase–1 (PDK-1, known primarily as a regulator of kinases) had the most restricted range, phosphorylating 4 substrates from 4 functional families.

We next examined the convergence of multiple kinases onto single sites (kinase convergence motif; Fig. 3D), which allows both redundancy and regulation by multiple ranges of upstream pathways. We found 66 (86%) of the 77 substrates and 129 (64%) of the 202 specific sites phosphorylated in the array were phosphorylated by more than one kinase (tables S7, S13, and S14). Although the majority of sites targeted by multiple kinases were phosphorylated by 2 to 5 kinases, a small number of "hub" sites were phosphorylated by 8 to 12 kinases (Fig. 5C). At the protein level, a set of highly phosphorylated substrates (hub substrates) that interacted with 10 or more kinases could also be identified (Fig. 5C). For example, the adaptor protein, insulin receptor substrate 1 (IRS1), a critical node in insulin signaling and cross talk point of different signaling cascades, was phosphorylated 58 times by 23 kinases with Ser^{24} phosphorylated by 9 kinases. These hubs, which are potentially key points of convergence between multiple signaling pathways, were distributed relatively evenly between functional classes of substrates. Thus, kinase convergence of multiple kinases upon a single site appears to be widespread in the postsynaptic proteome.

Although kinase families phosphorylated a large range of substrates, clustering proteins based on the density of kinase-substrate interactions indicated a broad pattern of organization. When the kinases were grouped according to their generic site or motif specificity (38) into tyrosine (Tyr), proline-directed (Pro), basophilic (Bas), acidophilic or phosphate-directed (Ac/Ph), and Other kinases (Fig. 5, A and B), the network was found to be composed of three modules enriched with Bas, Pro, and Tyr kinases, respectively. At the level of individual sites, channels and receptors predominated among targets of Bas kinases, whereas cytoskeletal proteins were most frequently phosphorylation targets of Pro kinases (Fig. 5A). Among multiply phosphorylated Ser/Thr sites, 71% (67 of 95) primarily interacted (>50% of interactions) with one kinase class. For example, glutamate receptor sites accounted for 30% of all sites primarily phosphorylated by Bas kinases ($P = 0.0002$) and none of the sites in G proteins and modulators were primarily phosphorylated by Pro kinases ($P = 0.007$).

The above observations concerning Ser/Thr kinases would appear to reflect the sequential organization of second messenger pathways coupled to neurotransmitter receptors. Many Bas kinases (such as CaMKII, PKA and PKC) are regulated by second messengers and can be thought of as lying at the top of kinase cascades, converting Ca^{2+},adenosine 3′,5′-monophosphate (cAMP) and other signals into changes in phosphorylation. Downstream components of cascades such as the ERK/MAPK pathway are typically Pro-directed and "Other" Ser/Thr kinases. Our observations suggest that feedback control of pathway activation (channels and receptors) is largely due to upstream (Bas) kinases, whereas downstream kinases primarily coordinate output changes in cell-biological processes underlying plasticity (for instance cytoskeletal organization).

At the synapse these relationships may be modulated by proteinprotein interactions, which organize kinases and their substrates into complex signaling units such as the NMDAR complex (NRC) of MASC (membrane-associated guanylate kinase associated signaling complex). Within the NRC/MASC interaction network (15), Bas kinases were on average 2.5 steps from the nearest receptor subunit, significantly closer than Pro-directed/Other Ser/Thr kinases, which were on average 3.6 steps from a receptor (Welch two-sample *t* test, $P = 0.026$). Thus, the sequential organization into upstream (Bas) and downstream Ser/Thr kinases appears to be reinforced by protein-protein interactions within neurotransmitter receptor complexes.

Additional patterns were observed at the level of convergence of kinase classes onto adjacent phosphorylation sites (paired convergence motif; Fig. 3E). Individual sites were first classified according to the type of kinase providing their major source of interactions

(for instance, Pro, Tyr), with those for which no single type provided more than 50% of interactions being classified as "mixed." The frequency with which pairs of classes occurred as adjacent sites was then compared to a random distribution. Same-class pairings were significantly enriched, notably Pro-Pro ($P < 10^{-4}$), Ac/Ph-Ac/Ph ($P = 0.003$) and Bas-Bas ($P = 0.01$). So not only do kinases from the same class converge on a similar set of substrates, they also converge onto adjacent sites within those substrates, allowing within-class modulation.

Bas kinases, the primary target for synaptic second messengers, also appeared to play a major role in between-class convergence onto adjacent sites, because Pro-Tyr ($P = 0.01$) and Pro-Ac/Ph ($P = 0.02$) pairings were significantly underrepresented. Thus, pairing of adjacent sites allows coordination within the functional units defined by kinase classes, and facilitates feed-forward regulation (through Bas kinases) by second messengers.

Multiphosphorylation site switches

Previous studies of multiply phosphorylated sequences have uncovered interactions between sites with the presence of a phosphate on one site influencing the probability of phosphorylation at another (primed convergence motif; Fig. 3G) (39, 40). For example, enhancement of GSK3β phosphorylation has been widely described, with several kinases being reported to prime GSK3β activity. These include cyclin-dependent kinase 5 (CDK5) that primes GSK3β to phosphorylate Tau and collapsin responsive mediator protein–2 (CRMP2) (41, 42); PKA primes GSK3β to phosphorylate Tau (43); dual-specificity tyrosine-phosphorylated and regulated kinases (DYRK) prime GSK3β to phosphorylate eIF2Bε (44); and GSK3β primes itself to phosphorylate CRMP2 (45). Inhibitory interactions have also been reported; for instance, increased phosphorylation of IRS1 Tyr^{608} after insulin receptor stimulation correlates with decreased in vivo phosphorylation of IRS1 S612 by MAPK (46).

It is not clear whether primed convergence is restricted to a few key proteins or is widespread. We designed a second set of arrays in which 200 sequences from multiple phosphorylated sequences were tested with seven different synaptic kinases (Fig. 6A and tables S15 and S16). For these analyses, we substituted serines, threonines, or tyrosines by their phosphorylated analogs in different combinations. Thus, we were able to quantify the level of phosphorylation of a particular site when an adjacent residue was phosphorylated. Control peptides (in which Ser, Thr, and Tyr were substituted for Ala, Val, and Phe, respectively) were also included. We found that the presence of a phosphorylated site altered the phosphorylation in 66% of neighboring sites. Of these "primed" sites, 73% were inhibitory and 27% were enhancing (Fig. 6, B to D) and found in multiple classes of proteins. Amongst these sites, we observed specific examples supported by the literature, such as priming of GSK3β (40). These switching and priming events can act as molecular "coincidence detectors" and are widespread in the postsynaptic proteome.

Widespread regulation of protein interaction domains

To explore the extent of phosphorylation-dependent protein interactions, we exploited the site-specificity information on protein interaction domains revealed in our NMDA stimulation data sets. Overall, 81 (65%) NMDA-modulated proteins contained potential sites within binding ligand motifs (the sequences that bind protein interaction domains). The binding domain ligands predominantly regulated by NMDA stimulation were WW4 ($P < 0.0001$), Src homology 3 (SH3) type III ($P = 0.0025$), SH2 STAT5 ($P = 0.04$), and MYND (myeloid, Nervy, and DEAF-1) ($P = 0.04$) (fig. 2A). Cytoskeletal proteins harbored 42% of phosphopeptides containing WW motifs and 47% with SH3 motifs (both associated with proline-directed kinases) ($P = 0.00001$ and 0.007, respectively). Transcription and

Translation proteins harbored 35% of peptides with 14-3-3 motifs ($P = 0.001$); and MAGUKs, Adaptors, and Scaffold harbored 25% of peptides with FHA (forkhead-associated) motifs ($P = 0.02$). Moreover, there was a close correspondence between individual kinase classes and the types of binding interaction that they regulate. Taking the set of PPPArray sites within binding domain ligand motifs, we found that 70% of Ser/Thr sites in SH3 motifs and 50% in WW motifs were primarily phosphorylated by Pro kinases ($P = 0.0001$ and $P = 0.005$, respectively). Fifty percent of Ser/Thr sites in FHA motifs were unique to Ac/Ph kinases ($P = 0.008$)and 55% Ser/Thr sites in 14-3-3 motifs were unique to Bas kinases ($P = 0.01$). Seventy percent of all Tyr sites were found in SH2 motifs ($P = 0.00005$). Reflecting the abundance of cytoskeletal proteins among substrates of Pro kinases, SH3 ligand motifs overlapping phosphorylated sites were present in 60% of cytoskeletal proteins studied in the array ($P = 0.004$). These data indicate that phosphorylation-dependent regulation of protein-protein interactions is widespread with different kinase classes modulating different subsets of interactions and reshaping the PSD.

DISCUSSION

Dynamic PSD phosphoproteome networks

Using large-scale proteomic approaches, we find that neurotransmitter receptors initiate signaling in overlapping networks of hundreds of phosphorylation sites on more than 100 postsynaptic proteins. We identified multiple levels of network organization constructed from a set of phosphorylation motifs or building blocks that define wiring of the network. This organization included regulatory switches for enhancing and inhibiting signaling as well as hubs and signal convergence points. Multiple disease proteins mapped onto these signaling networks, which are modulated by therapeutic drugs that engage receptors driving these networks. The postsynaptic proteome networks provide a fresh view of the molecular complexity of synapse function that reveals an elaborate circuitry built on simple motifs with combinatorial and computational features.

What property does this computational machinery provide and why do synapses require such elaborate molecular circuitry? These networks provide a framework for the transmission of information from a single neurotransmitter receptor to numerous “output” proteins (receptors, channels, structural, translational regulation, signaling). Second, the network allows these sets of proteins to be orchestrated. Third, multiple kinases and convergence mechanisms provides robustness and resilience to perturbation of a single node in the network, such as a specific kinase, site, or substrate (47). Fourth, the priming seen within multiple phosphorylated sites allows coincidence detection and switching. For example, NMDAR-mediated phosphorylation of site 1 in a pair of sites may interfere or enhance the ability of site 2 to be phosphorylated by a kinase driven by the dopamine receptor. In addition to modulating specific substrates, these priming switches may control specific subnetworks of functional proteins (with different physiological outcomes). Other network mechanisms include feedback (for instance, kinase auto- and transphosphorylation) and forms of regulatory cross talk. These mechanisms allow receptors individually, in combination, or in different temporal sequences to activate overlapping networks that orchestrate and differentially regulate a combination of effector substrates, which modulate many properties of the nerve cell and produce a range of physiological outcomes.

Network regulation of synaptic plasticity

Mutations or pharmacological perturbations show that many synaptic proteins are required for induction of long-term potentiation (LTP) of synaptic transmission (5, 15, 48-53) (www.genes2cognition.org/db) (54). These LTP proteins are found in a wide range of functional classes including receptors, scaffolding proteins, enzymes, cytoskeletal proteins,

and transcriptional regulators, among others. Our data link together these molecules into a functional signaling network and provides a framework for understanding their interrelationships.

The large repertoire of phosphorylation sites presents potential for combinatorial patterns of phosphorylation. Using stimulation conditions that activate different kinase pathways, we observed distinct combinations of phosphorylation patterns on multiple substrates (10 sites on four proteins) and unique combinations within a single protein (GluR1 S831, T840, S845) (table S16). This indicates that the presence of a phosphate on one site does not necessarily correlate with the physiological state of the synapse (e.g., LTP or LTD) and that a combinatorial code of sites is likely more relevant. This is supported by data on GluR1 phosphorylation where increases in phosphorylation of Ser^{845} and of Ser^{831} correlate with either LTP or LTD (55–57). An advantage of this combinatorial phosphorylation code is that an enormous number ($>2^{100}$) of possible physiological states could arise from the network, although our findings indicate that the number of distinct combinations that occur will be constrained.

Specific combinations of phosphorylation are likely to map onto short-term (~minutes) and long-term (hours) processes that confer precise tuning of synaptic physiology and its metaplasticity (58, 59). For example, three types (N, L, and R) of calcium channel, each with differing kinetics, were modulated by NMDAR (table S15) along with other channels that influence synaptic currents. Another postsynaptic kinase-dependent mechanism of long-term maintenance of LTP involves the synthesis of PKMζ (the active form of PKCζ), postulated as a site of convergence and integration for multiple kinases (60). The role of PKMζ in LTP maintenance has been well described (61); however, its targets remain elusive. Our peptide arrays showed that PKCζ phosphorylated 25 different substrates among different functional classes, including glutamate receptor subunits (NR1, GluR1, GluR2, mGluR4a, mGluR7a), scaffold proteins (PSD-95), kinases (PKC-ι), phosphatases, (PP1C-A), and others (tables S6 to S8), which together may regulate LTP maintenance. We also found proteins not previously implicated in plasticity, including several splicing factors (table S15), which is of interest because recent evidence suggests a role for localized splicing in dendrites (62).

Implications for learning and memory

The electrophysiological paradigm of LTP, which is the prevailing model for learning and memory, is based on synapses shifting between a weak and a strongstate (63, 64). Computational models, however, indicate that simple two-state synapses are poor at storing memories and vulnerable to erasure (12, 13). Using models in which synapses exist in a higher number of physiological states, Fusi and Abbott found improved memory performance with even a few additional states (they chose 15) (13). Our multistate phosphoproteome networks could provide such states and, thus, improved memory performance. Our data are also compatible with known molecular mechanisms of metaplasticity, the “plasticity of synaptic plasticity” (58, 59). Metaplasticity models introduce additional functional states and transitions between them. For example, the ability of a synapse to strengthen or weaken is influenced not only by the immediate activity that induces LTP or LTD, but also by its prior history of activity. Kinases and phosphatases and the receptors that activate postsynaptic networks are known to regulate metaplasticity. These physiological models of metaplasticity have identified relatively few forms of synaptic plasticity (<20) (65) compared with postsynaptic phosphoproteome states. Future modeling studies could consider the far higher numbers of states of molecular networks as well as the role of subnetworks with distinct properties.

We propose that a single synapse exploits the molecular complexity of postsynaptic proteomes to represent and process a wide range of information states reflecting the incoming information from neurotransmitters as well as the prior history (memory) of the synapse. The outcome is to change the states of the molecular network across a vast range, represented in the combinations of phosphorylation. These multistate networks could provide the multistate mechanisms that were shown to confer improved memory storage and recall over simpler synapse models (12, 13)

Synapse phosphoproteome networks and disease

These network mechanisms of learning and plasticity raise the possibility that network disruption may arise in diseases of cognition. Of the NMDA-modulated proteins identified in our study, 21 have been implicated in various disorders, including AD, Huntington's and Parkinson's disease, schizophrenia, and autism (table S17). The role of phosphorylation in AD illustrates many of the network regulatory features identified earlier. AD is a common neurodegenerative disorder characterized by the presence of extracellular amyloid plaques and intracellular neurofibrillary tangles largely composed of hyperphosphorylated microtubule-associated protein tau. Of the NMDA-modulated proteins implicated in AD (CRMP2, GSK3β, Map1b, Map2, tau, Ndrg2, P140, Itsn1), most are involved in microtubule/ cytoskeletal dynamics. CRMP2 regulates microtubule formation by binding tubulin. This interaction is regulated by GSK3β phosphorylation of CRMP2 at Thr^{509}/ Thr^{514}/Ser^{518}, subject to priming by Cdk5 at Ser^{522} (42). Cdk5 also primes GSK3β phosphorylation of tau (66). Consistent with this, we found NMDAR stimulation increased inhibitory phosphorylation of GSK3β and led to the dephosphorylation of CRMP2 peptides containing Thr^{514} and Ser^{518} (and also Ser^{522}). Hyperphosphorylation of CRMP2 at Thr^{509},Thr^{514},Ser^{518},and Ser^{522} is present in AD, preceding the appearance of neurofibrillary tangles and amyloid plaques in rodent models of the disease (67). Because proteins involved with many nervous system diseases are within these postsynaptic signaling networks, the use of NMDAR antagonists or specific modulators of kinases or phosphatases could potentially be of therapeutic benefit in a number of neurological disorders.

METHODS

Hippocampal slice stimulation

Mice were killed by cervical dislocation in accordance with Schedule 1 to the UK Animals (Scientific Procedures) Act 1986. Hippocampal slices from 12- to 14-week-old 129S5/ SvEvBrd mice bred at the Wellcome Trust Sanger Institute were prepared as described (68) and in supplemental data (table S17). Slices were incubated with 20 μM NMDA(3min),50 μM forskolin (15 min), wortmannin 200 nm (40 min), 10 μM phorhol 12,13-dibutyrate (PdBu) (15 min), 10 μM SB415286 (90 min), 10 μM KN-62 (30 min), and 20 μM U0126 (40 min). All drugs were from Tocris Cookson Ltd (Bristol, UK). Postsynaptic density fractions were prepared as described (supplemental data). For MS experiments, hippocampal slices from the same animals were treated with NMDA or untreated, in six independent assays, for a total of 24 mice. The Triton X-100 insoluble fraction was isolated from NMDA-treated (20 mM NMDA for 3 min) and control mouse hippocampal slices. This fraction (3 mg) was solubilized in 1% deoxycholate, treated with TCEP [tris(2-carboxyethyl)phosphine] and digested with trypsin for 4 hours. Desalted peptides were methyl-esterified for 2 hours and phosphopeptides were isolated using gallium IMAC as described previously (7).

LC-MS/MS and MS3 analysis

Phosphopeptides were separated with a 2-hour RP gradient on a PepMap C18 column (75-μm inner diameter × 15 cm; LC Packings). Phosphopeptides purified from control and

NMDA-stimulated samples were analyzed using a hybrid linear ion trap–Fourier transform ion cyclotron resonance (FTICR) mass spectrometer which was operated with a cycle of one MS (in the FTICR cell) and three MS/MS scans and up to three neutral loss triggered MS3 scans (in the ion trap) in parallel taking less than 2 s.

All data were processed by BioWorks v3.2 (Thermo) and searched using Mascot against a nonredundant, nonidentical mouse sequence database generated in-house. Static modification of methyl DE and C-term and variable modification of Oxidation (M), Acetyl (protein N-term), Phospho (STY), and Phospho PL (ST) for MS3 spectra were used for database searching with a peptide tolerance of 0.5 Da and an MS/MS tolerance of 0.8 Da. False discovery rates determined by Mascot decoy searches and empirical analyses of the distributions of mass deviation and Mascot Ion Score were used to establish score and mass accuracy filters. The mascot homology threshold was found to produce a 1% false discovery rate (FDR) by decoy searching and as such was adopted as first-pass filter of the data. Empirical analysis of high-quality MS2 spectra also showed 89% of these peptides fell within a 25-ppm window of the calculated mass, and as such, this mass accuracy value was used as an additional measure of confidence for MS2 peptide identification. Decoy searching also revealed that the identification of MS2-MS3 pairs by chance alone was unlikely (FDR 0%). As such, any MS2-MS3 pairs identified were accepted as true positive identifications.

As MS data are acquired in the FTICR cell, high accuracy and continuous measurement of the mass and intensity of phosphopeptides eluting into the mass spectrometer are achieved. The area under each peptide peak as monitored in the MS survey chromatogram is indicative of its abundance and comparison of peak areas for each phosphopeptide in the control and NMDA experiments provides a quantitative measure of differential phosphopeptide abundance based on multiple data points. Phosphopeptide identifications were performed with MASCOT and scan numbers of approved phosphopeptide were matched to phosphopeptide peaks in the MS survey chromatogram. Peak area calculations were made with BioWorks version 3.2 (Thermo Fisher) using ICIS peak detection. MS data processing and analysis are described in the supplementary methods section.

Peptide array phosphorylation assays

Jerini Phosphosite detector peptide arrays (Jerini Peptide Technologies, Gmbh) were used to analyze 600 peptide sequences corresponding to 91 PSD proteins with the use of previously described methods (7) and Supplemental Data. For priming arrays, additional phosphorylated sequences and corresponding controls were included in a 300-peptide array (table S18) probed with PKCα,CKI,ERK2,TBK1, Fyn, GSK3β, and p38α. (For protein kinase list, see table S18.)

Overlap between sets of molecules

The statistical significance of an overlap between two sets of molecules was calculated with the method of Pocklington et al.(15). This was used to analyze the phosphorylation of substrate classes (and sites within functional motifs) by kinase classes. See Supplemental Data for further details and table S19.

Convergence of kinase classes onto adjacent sites

Each site phosphorylated in the array was first classified according to the kinase class (Bas, Pro, Ac/Ph, Other, Tyr) providing >50% of its interactions, those in which no class predominated being classified as mixed. All pairs of adjacent sites (within 10 amino acids of each other) were identified, and the number of pairings of each classification was counted. Site classifications were randomly permuted 10,000 times, and the number of pairings in

each permutation was counted. The probability ρ(*m*)of a pairing occurring *m* times was estimated as N_m/10,000, where N_m was the number of permutations in which *m* pairings were found. Values quoted in the text sum over all ρ(*m*) for which ρ(*m*) ≤ ρ(*a*) (i.e., the probability of a number of pairings as or less likely than *a*), where *a* is the actual number of pairings.

Motifs overlapping phosphorylation sites

The amino acid sequence of each substrate was randomly permuted, keeping the location of phosphorylation sites constant. Regular expression matching was then used to count the number of phosphorylation sites present in each type of motif. Recording the results of 10,000 such random permutations, we estimated the probability of a motif occurring *m* times as N_m/10,000. For *m* greater (less) than the expected number occurrences, N_m is the number of random permutations in which the motif occurred *m* or more (less) times. An identical procedure was used to analyze the number of modulated peptides containing potential phosphorylation sites within functional motifs.

Footnotes

*To whom correspondence should be addressed. sg3@sanger.ac.uk

SUPPLEMENTARY MATERIALS

www.sciencesignaling.org/cgi/content/full/2/68/ra19/DC1

Materials and Methods

Fig. S1. In vivo validation of peptide arrays.

Fig. S2. Phosphorylation of protein interaction domains and motifs.

Table S1. Phosphopeptide identifications by LC-MS/MS and MS3.

Table S2. Summary of phosphorylation states identified in each phosphopeptide.

Table S3. List of NMDA-modulated proteins and their functional classification.

Table S4. Analysis of glutamate receptor phosphorylation.

Table S5. NMDA-modulated proteins linked to disease.

Table S6. Known (in vivo) phosphorylation sites used in peptide arrays.

Table S7. Phosphorylation of other sites in peptide array.

Table S8. Additional phosphorylation sites in synaptic proteins.

Table S9. Protein name and functional classification of substrates represented in peptide array assays.

Table S10. Protein sequences of substrates used in peptide arrays.

Table S11. Protein kinases used in peptide arrays.

Table S12. Peptide array quantitation.

Table S13. Phosphorylation of known in vivo sites tested in peptide array.

Table S14. Phosphorylation of sequences with nondetermined phosphorylation sites.

Table S15. Phosphopeptide priming arrays.

Table S16. List of sequences tested in phosphopeptide priming arrays.

Table S17. Antibodies used in Western blot assays.

Table S18. Recombinant kinases used in peptide arrays.

Table S19. Kinase-kinase phosphorylation map of protein kinases used in peptide array assays.

References

Acknowledgments

This work was supported by the Wellcome Trust (M.O.C., M.V.K., S.S., M.D.R.C, J.S.C., and S.G.N.G.), Human Frontiers Science Program (M.P.C.), Medical Research Council (A.J.P.), and EU FP6 (R.T.U.). We thank N. Afinowi and V. J. Robinson for technical assistance; J. D. Armstrong, T. J. O'Dell, and members of the Genes to Cognition team for input; A. Enright for Fig. 4; and J. V. Turner for editorial assistance.

REFERENCES AND NOTES

1. Kandel ER. The molecular biology of memory storage: A dialogue between genes and synapses. Science. 2001; 294:1030–1038. [PubMed: 11691980]
2. Shepherd JD, Huganir RL. The cell biology of synaptic plasticity: AMPA receptor trafficking. Annu. Rev. Cell Dev. Biol. 2007; 23:613–643. [PubMed: 17506699]
3. Sheng M, Kim MJ. Postsynaptic signaling and plasticity mechanisms. Science. 2002; 298:776–780. [PubMed: 12399578]
4. Collins MO, Husi H, Yu L, Brandon JM, Anderson CN, Blackstock WP, Choudhary JS, Grant SG. Molecular characterization and comparison of the components and multiprotein complexes in the postsynaptic proteome. J. Neurochem. 2006; 97:16–23. [PubMed: 16635246]
5. Husi H, Ward MA, Choudhary JS, Blackstock WP, Grant SG. Proteomic analysis of NMDA receptor-adhesion protein signaling complexes. Nat. Neurosci. 2000; 3:661–669. [PubMed: 10862698]
6. Greengard P. The neurobiology of slow synaptic transmission. Science. 2001; 294:1024–1030. [PubMed: 11691979]
7. Collins MO, Yu L, Coba MP, Husi H, Campuzano I, Blackstock WP, Choudhary JS, Grant SG. Proteomic analysis of in vivo phosphorylated synaptic proteins. J. Biol. Chem. 2005; 280:5972–5982. [PubMed: 15572359]
8. Munton RP, Tweedie-Cullen R, Livingstone-Zatchej M, Weinandy F, Waidelich M, Longo D, Gehrig P, Potthast F, Rutishauser D, Gerrits B, Panse C, Schlapbach R, Mansuy IM. Qualitative and quantitative analyses of protein phosphorylation in naive and stimulated mouse synaptosomal preparations. Mol. Cell. Proteomics. 2007; 6:283–293. [PubMed: 17114649]
9. Trinidad JC, Specht CG, Thalhammer A, Schoepfer R, Burlingame AL. Comprehensive identification of phosphorylation sites in postsynaptic density preparations. Mol. Cell. Proteomics. 2006; 5:914–922. [PubMed: 16452087]
10. Jordan JD, Landau EM, Iyengar R. Signaling networks: The origins of cellular multitasking. Cell. 2000; 103:193–200. [PubMed: 11057893]
11. Ma'ayan A, Jenkins SL, Neves S, Hasseldine A, Grace E, Dubin-Thaler B, Eungdamrong NJ, Weng G, Ram PT, Rice JJ, Kershenbaum A, Stolovitzky GA, Blitzer RD, Iyengar R. Formation of regulatory patterns during signal propagation in a Mammalian cellular network. Science. 2005; 309:1078–1083. [PubMed: 16099987]
12. Fusi S, Abbott LF. Limits on the memory storage capacity of bounded synapses. Nat. Neurosci. 2007; 10:485–493. [PubMed: 17351638]
13. Fusi S, Drew PJ, Abbott LF. Cascade models of synaptically stored memories. Neuron. 2005; 45:599–611. [PubMed: 15721245]
14. Blitzer RD, Iyengar R, Landau EM. Postsynaptic signaling networks: Cellular cogwheels underlying long-term plasticity. Biol. Psychiatry. 2005; 57:113–119. [PubMed: 15652868]
15. Pocklington AJ, Cumiskey M, Armstrong JD, Grant SG. The proteomes of neurotransmitter receptor complexes form modular networks with distributed functionality underlying plasticity and behaviour. Mol. Syst. Biol. 2006; 2 2006.0023.
16. Bromberg KD, Ma'ayan A, Neves SR, Iyengar R. Design logic of a cannabinoid receptor signaling network that triggers neurite outgrowth. Science. 2008; 320:903–909. [PubMed: 18487186]
17. Lee HK, Kameyama K, Huganir RL, Bear MF. NMDA induces long-term synaptic depression and dephosphorylation of the GluR1 subunit of AMPA receptors in hippocampus. Neuron. 1998; 21:1151–1162. [PubMed: 9856470]
18. Caenepeel S, Charydczak G, Sudarsanam S, Hunter T, Manning G. The mouse kinome: Discovery and comparative genomics of all mouse protein kinases. Proc. Natl. Acad. Sci. U.S.A. 2004; 101:11707–11712. [PubMed: 15289607]
19. Jordan BA, Fernholz BD, Boussac M, Xu C, Grigorean G, Ziff EB, Neubert TA. Identification and verification of novel rodent postsynaptic density proteins. Mol. Cell. Proteomics. 2004; 3:857–871. [PubMed: 15169875]

20. Peng J, Kim MJ, Cheng D, Duong DM, Gygi SP, Sheng M. Semiquantitative proteomic analysis of rat forebrain postsynaptic density fractions by mass spectrometry. J. Biol. Chem. 2004; 279:21003–21011. [PubMed: 15020595]
21. Reisberg B, Doody R, Stoffler A, Schmitt F, Ferris S, Mobius HJ. Memantine in moderate-to-severe Alzheimer's disease. N. Engl. J. Med. 2003; 348:1333–1341. [PubMed: 12672860]
22. Beister A, Kraus P, Kuhn W, Dose M, Weindl A, Gerlach M. The N-methyl-D-aspartate antagonist memantine retards progression of Huntington'sdisease. J. Neural. Transm. Suppl. 2004:117–122. [PubMed: 15354397]
23. Merello M, Nouzeilles MI, Cammarota A, Leiguarda R. Effect of memantine (NMDA antagonist) on Parkinson's disease: A double-blind crossover randomized study. Clin. Neuropharmacol. 1999; 22:273–276. [PubMed: 10516877]
24. Stone JM, Morrison PD, Pilowsky LS. Glutamate and dopamine dysregulation in schizophrenia—A synthesis and selective review. J. Psychopharmacol. 2007; 21:440–452. [PubMed: 17259207]
25. Bonsi P, Cuomo D, Picconi B, Sciamanna G, Tscherter A, Tolu M, Bernardi G, Calabresi P, Pisani A. Striatal metabotropic glutamate receptors as a target for pharmacotherapy in Parkinson's disease. Amino Acids. 2007; 32:189–195. [PubMed: 16715415]
26. Jenner P. Pharmacology of dopamine agonists in the treatment of Parkinson's disease. Neurology. 2002; 58:S1–S8. [PubMed: 11909980]
27. Li J, Zhu M, Manning-Bog AB, Di Monte DA, Fink AL. Dopamine and L-dopa disaggregate amyloid fibrils: Implications for Parkinson's and Alzheimer's disease. FASEB J. 2004; 18:962–964. [PubMed: 15059976]
28. Lipton SA. Paradigm shift in neuroprotection by NMDA receptor blockade: Memantine and beyond. Nat. Rev. Drug Discov. 2006; 5:160–170. [PubMed: 16424917]
29. Cohen P. The origins of protein phosphorylation. Nat. Cell Biol. 2002; 4:E127–E130. [PubMed: 11988757]
30. Sweatt JD. The neuronal MAP kinase cascade: A biochemical signal integration system subserving synaptic plasticity and memory. J. Neurochem. 2001; 76:1–10. [PubMed: 11145972]
31. Westphal RS, Tavalin SJ, Lin JW, Alto NM, Fraser ID, Langeberg LK, Sheng M, Scott JD. Regulation of NMDA receptors by an associated phosphatasekinase signaling complex. Science. 1999; 285:93–96. [PubMed: 10390370]
32. Peineau S, Bradley C, Taghibiglou C, Doherty A, Bortolotto ZA, Wang YT, Collingridge GL. The role of GSK-3 in synaptic plasticity. Br. J. Pharmacol. 2008; 153(Suppl. 1):S428–S437. [PubMed: 18311157]
33. Silva AJ, Paylor R, Wehner JM, Tonegawa S. Impaired spatial learning in α-calcium-calmodulin kinase II mutant mice. Science. 1992; 257:206–211. [PubMed: 1321493]
34. Migaud M, Charlesworth P, Dempster M, Webster LC, Watabe AM, Makhinson M, He Y, Ramsay MF, Morris RG, Morrison JH, O'Dell TJ, Grant SG. Enhanced long-term potentiation and impaired learning in mice with mutant postsynaptic density-95 protein. Nature. 1998; 396:433–439. [PubMed: 9853749]
35. Sprengel R, Suchanek B, Amico C, Brusa R, Burnashev N, Rozov A, Hvalby O, Jensen V, Paulsen O, Andersen P, Kim JJ, Thompson RF, Sun W, Webster LC, Grant SG, Eilers J, Konnerth A, Li J, McNamara JO, Seeburg PH. Importance of the intracellular domain of NR2 subunits for NMDA receptor function in vivo. Cell. 1998; 92:279–289. [PubMed: 9458051]
36. deSouza S, Ziff EB. AMPA receptors do the electric slide. Sci. STKE. 2002; 2002:PE45. [PubMed: 12407223]
37. Delgado JY, Coba M, Anderson CN, Thompson KR, Gray EE, Heusner CL, Martin KC, Grant SG, O'Dell TJ. NMDA receptor activation dephosphorylates AMPA receptor glutamate receptor 1 subunits at threonine 840. J. Neurosci. 2007; 27:13210–13221. [PubMed: 18045915]
38. Pinna LA, Ruzzene M. How do protein kinases recognize their substrates? Biochim. Biophys. Acta. 1996; 1314:191–225. [PubMed: 8982275]
39. Roach PJ. Multisite and hierarchal protein phosphorylation. J. Biol. Chem. 1991; 266:14139–14142. [PubMed: 1650349]
40. Cohen P, Frame S. The renaissance of GSK3. Nat. Rev. Mol. Cell Biol. 2001; 2:769–776. [PubMed: 11584304]

41. Li T, Hawkes C, Qureshi HY, Kar S, Paudel HK. Cyclin-dependent protein kinase 5 primes microtubule-associated protein tau site-specifically for glycogen synthase kinase 3β. Biochemistry. 2006; 45:3134–3145. [PubMed: 16519508]
42. Uchida Y, Ohshima T, Sasaki Y, Suzuki H, Yanai S, Yamashita N, Nakamura F, Takei K, Ihara Y, Mikoshiba K, Kolattukudy P, Honnorat J, Goshima Y. Semaphorin3A signalling is mediated via sequential Cdk5 and GSK3β phosphorylation of CRMP2: Implication of common phosphorylating mechanism underlying axon guidance and Alzheimer's disease. Genes Cells. 2005; 10:165–179. [PubMed: 15676027]
43. Augustinack JC, Schneider A, Mandelkow EM, Hyman BT. Specific tau phosphorylation sites correlate with severity of neuronal cytopathology in Alzheimer's disease. Acta Neuropathol. 2002; 103:26–35. [PubMed: 11837744]
44. Woods YL, Cohen P, Becker W, Jakes R, Goedert M, Wang X, Proud CG. The kinase DYRK phosphorylates protein-synthesis initiation factor eIF2Bε at Ser^{539} and the microtubule-associated protein tau at Thr^{212}: Potential role for DYRK as a glycogen synthase kinase 3-priming kinase. Biochem. J. 2001; 355:609–615. [PubMed: 11311121]
45. Yoshimura T, Kawano Y, Arimura N, Kawabata S, Kikuchi A, Kaibuchi K. GSK-3β regulates phosphorylation of CRMP-2 and neuronal polarity. Cell. 2005; 120:137–149. [PubMed: 15652488]
46. Bard-Chapeau EA, Hevener AL, Long S, Zhang EE, Olefsky JM, Feng GS. Deletion of Gab1 in the liver leads to enhanced glucose tolerance and improved hepatic insulin action. Nat. Med. 2005; 11:567–571. [PubMed: 15821749]
47. Grant SG, O'Dell TJ, Karl KA, Stein PL, Soriano P, Kandel ER. Impaired long-term potentiation, spatial learning, and hippocampal development in fyn mutant mice. Science. 1992; 258:1903–1910. [PubMed: 1361685]
48. Strack S, Colbran RJ. Autophosphorylation-dependent targeting of calcium/calmodulin-dependent protein kinase II by the NR2B subunit of the N-methyl-D-aspartate receptor. J. Biol. Chem. 1998; 273:20689–20692. [PubMed: 9694809]
49. Soderling TR, Chang B, Brickey D. Cellular signaling through multifunctional Ca^{2+}/calmodulin-dependent protein kinase II. J. Biol. Chem. 2001; 276:3719–3722. [PubMed: 11096120]
50. Barria A, Derkach V, Soderling T. Identification of the Ca^{2+}/calmodulin-dependent protein kinase II regulatory phosphorylation site in the α-amino-3-hydroxyl-5-methyl-4-isoxazole-propionate-type glutamate receptor. J. Biol. Chem. 1997; 272:32727–32730. [PubMed: 9407043]
51. Barria A, Muller D, Derkach V, Griffith LC, Soderling TR. Regulatory phosphorylation of AMPA-type glutamate receptors by CaM-KII during long-term potentiation. Science. 1997; 276:2042–2045. [PubMed: 9197267]
52. Mammen AL, Kameyama K, Roche KW, Huganir RL. Phosphorylation of the α-amino-3-hydroxy-5-methylisoxazole4-propionic acid receptor GluR1 subunit by calcium/ calmodulin-dependent kinase II. J. Biol. Chem. 1997; 272:32528–32533. [PubMed: 9405465]
53. Sanes JR, Lichtman JW. Can molecules explain long-term potentiation? Nat. Neurosci. 1999; 2:597–604. [PubMed: 10404178]
54. Croning MD, Marshall MC, McLaren P, Armstrong JD, Grant SG. G2Cdb: The Genes to Cognition database. Nucleic Acids Res. 2009; 37:D846–D851. [PubMed: 18984621]
55. Delgado JY, O'Dell TJ. Long-term potentiation persists in an occult state following mGluR-dependent depotentiation. Neuropharmacology. 2005; 48:936–948. [PubMed: 15857620]
56. Lee HK, Barbarosie M, Kameyama K, Bear MF, Huganir RL. Regulation of distinct AMPA receptor phosphorylation sites during bidirectional synaptic plasticity. Nature. 2000; 405:955–959. [PubMed: 10879537]
57. Vanhoose AM, Winder DG. NMDA and β1-adrenergic receptors differentially signal phosphorylation of glutamate receptor type 1 in area CA1 of hippocampus. J. Neurosci. 2003; 23:5827–5834. [PubMed: 12843287]
58. Abraham WC, Bear MF. Metaplasticity: The plasticity of synaptic plasticity. Trends Neurosci. 1996; 19:126–130. [PubMed: 8658594]
59. Abraham WC. Metaplasticity: Tuning synapses and networks for plasticity. Nat. Rev. Neurosci. 2008; 9:387. [PubMed: 18401345]

60. Kelly MT, Crary JF, Sacktor TC. Regulation of protein kinase Mζ synthesis by multiple kinases in long-term potentiation. J. Neurosci. 2007; 27:3439–3444. [PubMed: 17392460]

61. Pastalkova E, Serrano P, Pinkhasova D, Wallace E, Fenton AA, Sacktor TC. Storage of spatial information by the maintenance mechanism of LTP. Science. 2006; 313:1141–1144. [PubMed: 16931766]

62. Glanzer JG, Enose Y, Wang T, Kadiu I, Gong N, Rozek W, Liu J, Schlautman JD, Ciborowski PS, Thomas MP, Gendelman HE. Genomic and proteomic microglial profiling: Pathways for neuroprotective inflammatory responses following nerve fragment clearance and activation. J. Neurochem. 2007; 102:627–645. [PubMed: 17442053]

63. Bliss TV, Collingridge GL. A synaptic model of memory: Long-term potentiation in the hippocampus. Nature. 1993; 361:31–39. [PubMed: 8421494]

64. Montgomery JM, Madison DV. State-dependent heterogeneity in synaptic depression between pyramidal cell pairs. Neuron. 2002; 33:765–777. [PubMed: 11879653]

65. Malenka RC, Bear MF. LTP and LTD: An embarrassment of riches. Neuron. 2004; 44:5–21. [PubMed: 15450156]

66. Arioka M, Tsukamoto M, Ishiguro K, Kato R, Sato K, Imahori K, Uchida T. Tau protein kinase II is involved in the regulation of the normal phosphorylation state of tau protein. J. Neurochem. 1993; 60:461–468. [PubMed: 8419532]

67. Cole AR, Knebel A, Morrice NA, Robertson LA, Irving AJ, Connolly CN, Sutherland C. GSK-3 phosphorylation of the Alzheimer epitope within collapsin response mediator proteins regulates axon elongation in primary neurons. J. Biol. Chem. 2004; 279:50176–50180. [PubMed: 15466863]

68. Kopanitsa MV, Afinowi NO, Grant SG. Recording long-term potentiation of synaptic transmission by three-dimensional multi-electrode arrays. BMC Neurosci. 2006; 7:61. [PubMed: 16942609]

69. Newman ME, Girvan M. Finding and evaluating community structure in networks. Phys Rev E Stat Nonlin Soft Matter Phys. 2004; 69:026113. [PubMed: 14995526]

Europe PMC Funders Author Manuscripts

Europe PMC Funders Author Manuscripts

One-sentence summary: Analysis of protein phosphorylation patterns provides insight into the organization of molecular networks at the postsynaptic density.

Editor's Summary:

Patterning Postsynaptic Phosphorylation

The postsynaptic density of excitatory synapses in the mammalian brain—the initial site for integration of incoming information from the presynaptic neuron—contains over a thousand different proteins. Rather than investigating the effects of neurotransmitter signaling on a single pathway, Coba et al. explored the functional organization of these postsynaptic density proteins. Using a large-scale proteomic approach, they found that stimulation of different classes of neurotransmitter receptor affected the phosphorylation status of hundreds of phosphorylation sites in overlapping networks of postsynaptic density proteins. Identification of a set of regulatory phosphorylation motifs enabled them to construct a model of the molecular circuitry of the postsynaptic proteome, a crucial step in elucidating how postsynaptic neurons process incoming information.

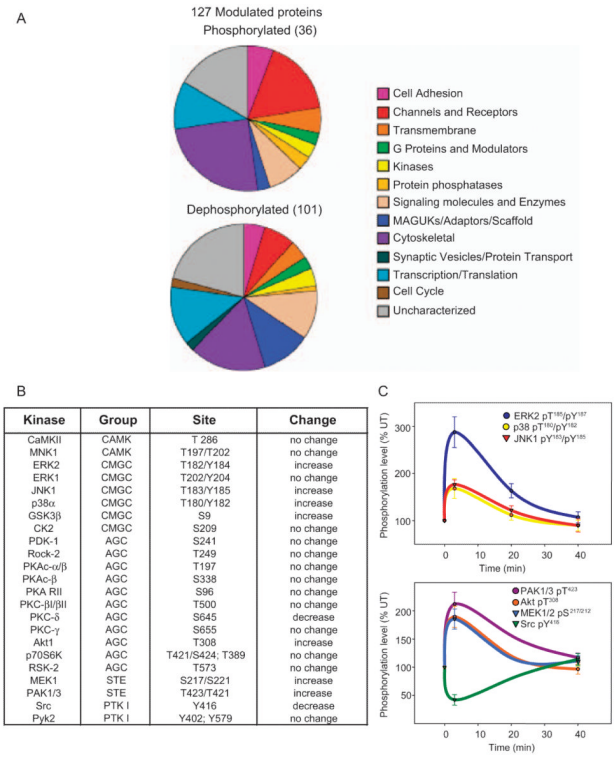

Kinase	Group	Site	Change
CaMKII	CAMK	T 286	no change
MNK1	CAMK	T197/T202	no change
ERK2	CMGC	T182/Y184	increase
ERK1	CMGC	T202/Y204	no change
JNK1	CMGC	T183/Y185	increase
p38α	CMGC	T180/Y182	increase
GSK3β	CMGC	S9	increase
CK2	CMGC	S209	no change
PDK-1	AGC	S241	no change
Rock-2	AGC	T249	no change
PKAc-α/β	AGC	T197	no change
PKAc-β	AGC	S338	no change
PKA RII	AGC	S96	no change
PKC-βI/βII	AGC	T500	no change
PKC-δ	AGC	S645	decrease
PKC-γ	AGC	S655	no change
Akt1	AGC	T308	increase
p70S6K	AGC	T421/S424; T389	no change
RSK-2	AGC	T573	no change
MEK1	STE	S217/S221	increase
PAK1/3	STE	T423/T421	increase
Src	PTK I	Y416	decrease
Pyk2	PTK I	Y402; Y579	no change

Fig. 1.

NMDA stimulation of hippocampal slices. (A) NMDA-mediated changes in the phosphorylation status of 127 proteins of the PSD (detected by MS). (B) NMDA-dependent modulation of 9 of 23 different kinases from five groups, detected by immunoblot 3 min after NMDAR stimulation. (C) Modulation of 7 kinases was assayed by immunoblotting with phosphospecific antibodies of hippocampal slice extracts after NMDA stimulation. Peak changes occurred between 3 and 5 min after stimulation, and phosphorylation returned to the basal state after 40 min.

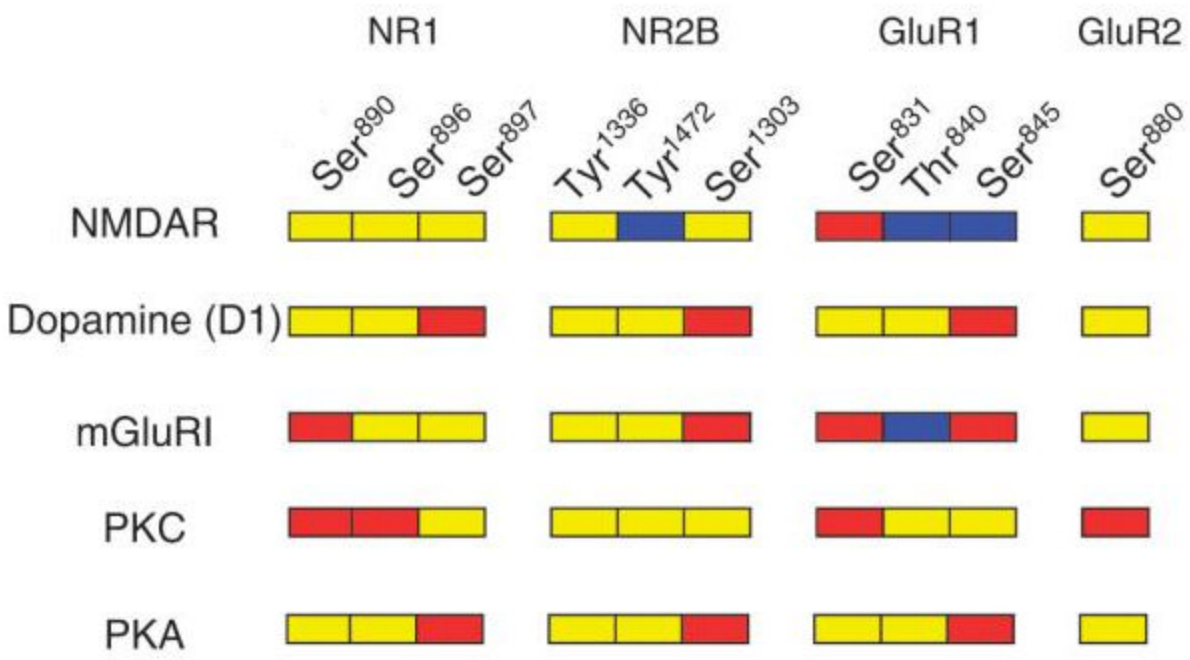

Fig. 2.

Overlapping networks driven by NMDA, mGlu and dopamine receptors, and PKA and PKC. Phosphorylation on NMDA (NR1, NR2B) and AMPA subunits (GluR1, GluR2) (10 total) was monitored with phosphospecific antibodies after stimulation. The following receptors were stimulated with the indicated agonists: NMDAR: NMDA (20 μM), dopamine D1–like agonist (6-Cl-PB, 50 μM), mGluR (DHPG, 50 μM). PKA was activated directly with forskolin (50 μM) and PKC with PdBu (10 μM). Red: increase in phosphorylation compared to control; yellow: no change; blue: decrease.

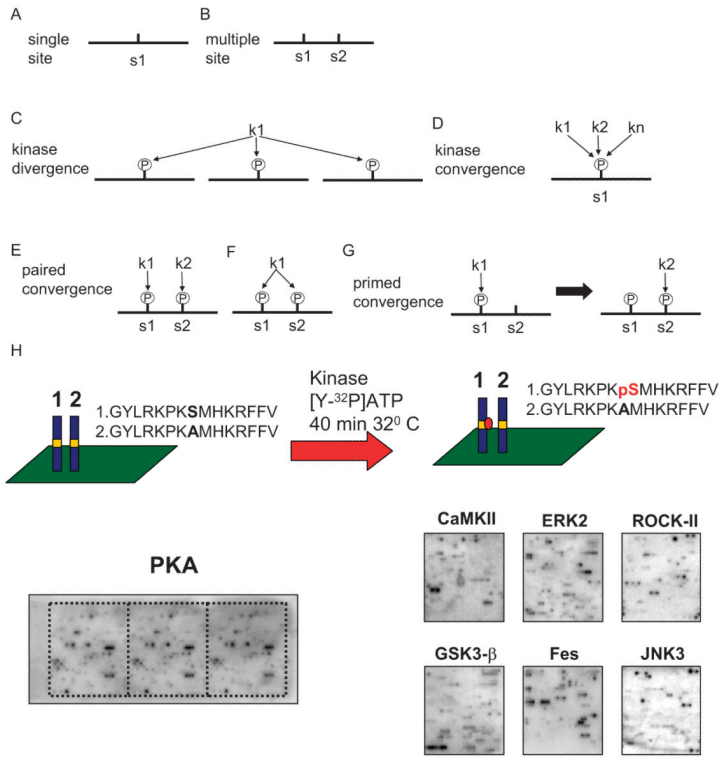

Fig. 3.

Regulatory motifs and mapping of kinase sites. (**A** and **B**) Sequences contain single (A) or multiple (B) sites and regulatory motifs representing different phosphorylation events were described by their substrate-kinase interactions (**C** to **G**). s, substrate. (C) Kinase divergence: a single kinase can phosphorylate multiple independent sequences. k, kinase, P, phosphate. (D) Kinase convergence: single site sequence phosphorylated by multiple kinases. (E) Paired convergence: multiple site sequence with two different kinases phosphorylating each site. (F) Paired convergence: multiple site sequence with a single kinase phosphorylating each site. (G) Primed convergence: phosphorylation sites within 10 amino acids of each other presenting priming effects in which the presence of phosphate on site 1 influences phosphorylation of site 2. (H) Scheme for kinase site identification on peptide substrates. Fifteen amino acid peptides containing a phosphorylation site and a control peptide (for instance, in which a serine site was substituted with an alanine) were immobilized and phosphorylated on glass slides. Representative phosphoimages of ^{32}P-labeled arrays after kinase reactions with PKA (triplicate samples) and six other kinases. JNK3, c-Jun N-terminal kinase 3 Fes, *c-fps/fes* proto-oncogene tyrosine kinase. ROCK-II, Rho-associated kinase 2.

Europe PMC Funders Author Manuscripts

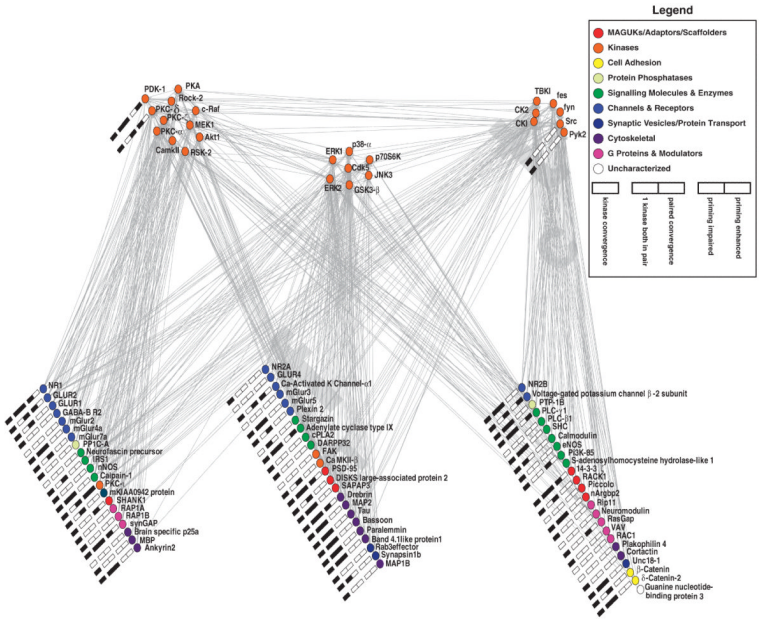

Fig. 4.

Postsynaptic phosphoproteome network. The network was constructed by linking kinases to their respective substrates, which include other kinases. We separated the network into groups of proteins (with a high density of links within each group and a lower density of links between different groups) with the use of an unsupervised clustering algorithm. In the diagram, each group was separated into two levels (one level containing kinases, the other containing substrates) for ease of viewing. Kinases were not randomly distributed within this clustering: One cluster was enriched with basophilic kinases (although it also contained other kinases), another was enriched with proline-directed kinases, and so forth. Thus, the network of phosphorylation interactions shows evidence of a broad organizational pattern based on kinase classes, although there is cross talk. For each substrate, phosphorylation sites were categorized into regulatory motifs (Fig. 3). Adjacent to each substrate is a "barcode" composed of five boxes (shaded either black or white) indicating the presence (black) or absence (white) of particular regulatory motifs within that substrate. Kinases (top) and substrate (bottom) interactions were graphed (gray lines) and clustered with the algorithm of Newman and Girvan (69). Functional classes of substrates are shown (colored symbols, see key).

Europe PMC Funders Author Manuscripts

A

Site/motif specificity	Kinase	*n* site	*n* substrate	Most phosphorylated family	% sites
Basophilic (Bas)	CaMKII	19	16	Channels/Receptors	26
	Akt1	17	14	Channels/Receptors	35
	PKC-α	30	25	Channels/Receptors	20
	PKC-δ	25	20	Channels/Receptors	28
	PKC-ζ	25	19	Channels/Receptors	32
	p70S6K	30	21	Signaling molecules & enzymes	37
	PKA	33	29	Channels/Receptors	21
	Rock-2	17	14	Signaling molecules & enzymes	35
	RSK2	29	23	Signaling molecules & enzymes	28
Proline-directed (Pro)	ERK1	56	27	Cytoskeletal	25
	ERK2	37	36	Cytoskeletal	32
	Cdk5	34	24	Cytoskeletal	26
	JNK3	8	8	Signaling molecules & enzymes	25
	p38-α	36	25	Cytoskeletal	33
Acidophilic/phosphate directed (Ac/Ph)	CK2	11	8	Signaling molecules & enzymes	27
	CK1	55	36	Signaling molecules & enzymes	31
	GSK3-β	32	22	Signaling molecules & enzymes	27
Other	c-raf	14	11	Signaling molecules & enzymes	29
	MEK1	16	10	Kinases	31
	PDK-1	5	4	Kinases	40
	TBK1	43	28	MAGUKs/Adaptors/Scaffolders	26
Tyrosine (Tyr)	fyn	34	22	Signaling molecules & enzymes	32
	Src	34	22	Signaling molecules & enzymes	32
	Pyk2	34	21	Signaling molecules & enzymes	35
	fes	49	27	Signaling molecules & enzymes	33

B

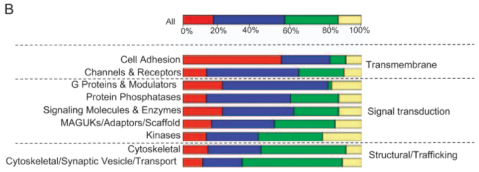

C

Hub protein	Total	Hub site	n kinase/site	family
IRS1	23	S24	9	Signaling molecules & enzymes
PSD-95	20			MAGUKs/Adaptors/Scaffolders
GluR2	19			Channels/Receptors
Calpain-1	18	S379	12	Signaling molecules & enzymes
Calpain-1	18	T380	12	Signaling molecules & enzymes
Shank1	18			MAGUKs/Adaptors/Scaffolders
14-3-3 ζ	17	S58	10	Signaling molecules & enzymes
PKC-δ	15			Kinases
RasGap	13			Signaling molecules & enzymes
Bassoon	13			Cytoskeletal
PKC-	12			Kinases
GluR1	12			Channels/Receptors
cPLA2	11			Signaling molecules & enzymes
Drebrin	11	S140	11	Cytoskeletal
NR2βB	11			Channels/Receptors
PTP-1B	10			Protein Phosphatases
NR1	10	S889	8	Channels/Receptors
DARPP32		T34	9	Signaling molecules & enzymes
mGlur4a		S859	9	Channels/Receptors
mGlur7a		S862	8	Channels/Receptors

Fig. 5.

Distribution of kinase types, sequence motifs, classes of proteins and hubs in phosphorylated substrates. (**A**) Protein kinases were grouped by their preferred sequence specificity into five categories: basophilic (blue), proline-directed (green), acid and phosphate-directed (red), other (yellow), and tyrosine (purple). The number of sites phosphorylated by each kinase is shown, with the top substrate class targeted by each kinase and the percentage of the total number of phosphorylated sites detected. Columns indicate specific kinases (kinase), the total number of substrate phosphorylation sites (*n* site), and total number of protein substrates (n substrate) and preferred functional class of substrates (most phosphorylated family) with the percentage of that substrate shown (% sites). (**B**) Proportion of (peptide array) Ser/Thr phosphorylation events due to each kinase group (color coding as in A). Shows percentage of all Ser/Thr phosphorylation events and of events for each functional class of substrate. Note uneven distribution, with proline-directed kinases showing a preference for structural and trafficking substrates. (**C**) Hubs or highly phosphorylated substrates phosphorylated by 10 or more kinases. Total, number of kinases that phosphorylate that protein. N kinase/site, number of kinases that phosphorylate the Hub site.

Europe PMC Funders Author Manuscripts

Europe PMC Funders Author Manuscripts

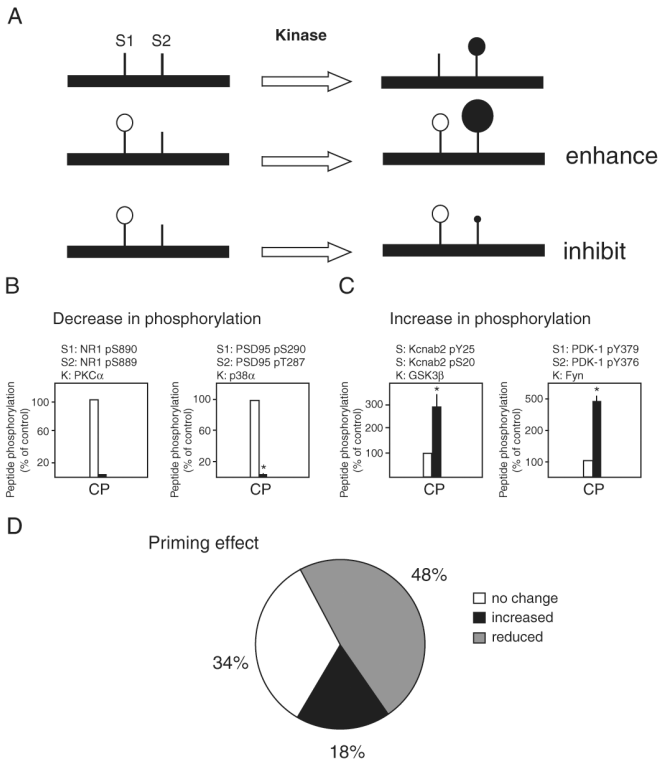

Fig. 6.

Phosphorylation site interactions on priming arrays. (**A**) Interaction between phosphorylation sites in multiple phosphorylated sequences. Peptides with two phosphorylation sites (S1, site 1; S2, site 2) are represented (top left) and, after kinase reaction that is specific to site 2, we measured the incorporation of ^{32}P (black circle, top right). Peptides synthesized with a phosphate on site 1 (white circle, lower left) are used in the same kinase reaction and the site 2 incorporation measured (black circle, lower right). An increase or decrease in site 2 phosphorylation is indicated by the larger or smaller black symbol. (**B**) Two examples (NR1, PSD95) in which introduction of a phosphorylation site into a sequence (S1) decreased the total phosphorylation of a second phosphorylation site (S2). Each histogram shows the site 2 phosphorylation (% control) for peptide control (C, corresponds to top right peptide in A) and its primed variant (*P*, corresponds to bottom right peptide in A) for the representative kinase (k). (**C**) In contrast to (B), two examples (Kcnab2, PDK-1) in which the introduction of a phosphorylation site into a peptide sequence (S1) increased the total phosphorylation of a second phosphorylation site (S2). (D) The overall effect of priming on all peptides shows that 34% had no effect, whereas 48% were inhibitory and 18% were enhancing.